Effect of Increasing Inhibitory Inputs on Information Processing Within a Small Network of Spiking Neurons

Roberta Sirovich[1,2], Laura Sacerdote[1], and Alessandro E.P. Villa[2]

[1] Department of Mathematics, University of Torino
Via Carlo Alberto 10, 10123 Torino, Italy
Roberta.Sirovich@unito.it, Laura.Sacerdote@unito.it
[2] Neuroheuristics Research Group
University Joseph Fourier Grenoble 1
Equipe NanoNeurosciences Fondamentales et Appliques
Grenoble Institut des Neurosciences - U 836 Inserm - UJF -CEA France
Alessandro.Villa@ujf-grenoble.fr

Abstract. In this paper the activity of a spiking neuron A that receives a background input from the network in which it is embedded and strong inputs from an excitatory unit E and an inhibitory unit I is studied. The membrane potential of the neuron A is described by a jump diffusion model. Several types of interspike interval distributions of the excitatory strong inputs are considered as Poissonian inhibitory inputs increase intensity. It is shown that, independently of the distribution of the excitatory inpu, they are more efficiently transmitted as inhibition increases to larger intensities.

1 Introduction

The model we consider here has been at first introduced in [3] and deeply analyzed in [4]. There we observed that as the importance of the inhibitory inputs increases, the model responds with higher efficiency to excitatory inputs. In this paper we investigate on the robustness of such a result. We test whether the property of the model we observed in [4] is due to the choice of the excitatory interspike interval distribution or if it is intrinsic of the structure of the model. To this purpose, we consider four different alternative excitatory interspike interval distributions, each one of them showing different features and different effects on the model. And we study the efficiency of the excitatory input transmission as the inhibition increases. The results discussed in the following allow to conclude that the behavior observed in [4] can be generalized to a larger variety of excitatory interspike interval distribution. So that it is possible to state that the result is due to the structure of the model.

F. Sandoval et al. (Eds.): IWANN 2007, LNCS 4507, pp. 23–30, 2007.

2 The Model

The equations. The membrane potential of a neuronal cell is described by the jump diffusion process $V = \{V_t, t \geq 0\}$, i.e. the random variable V_t gives the probabilistic description of the membrane potential at time t. Each time the process V crosses a given constant threshold S, we assume that the cell fires and gives an output spike. Hence the times of firing of the cell are given by the successive values taken by the random variable $T = \inf\{t \geq 0 : V_t \geq S\}$, $V_0 < S$, that is the so called first passage time of the stochastic process across the threshold S. We assume that the process V is given by the following equation

$$V_t = V_0 + \int_0^t \left(-\frac{1}{\theta}V_s + \mu\right) ds + \sigma W_t + a_+ N_t^+ + a_- N_t^-, \tag{1}$$

where $V_0 < S$, $a_+ > 0$ and $a_- < 0$ are constant, the processes $N^+ = \{N_t^+, t \geq 0\}$ and $N^- = \{N_t^-, t \geq 0\}$ are two independent counting processes, $\mu \in \mathbf{R}$, $\theta > 0$, $\sigma > 0$ and the process $W = \{W_t, t \geq 0\}$ is a standard Brownian motion. The process V is called a jump diffusion process since it is the sum of a continuous part, where we recognize the Ornstein-Uhlenbeck diffusion process, and two counting processes, the processes N^+ and N^-. So that V has continuous sample paths except in the points of discontinuity corresponding to the times of occurrence of events in the processes N^+ and N^-, where upward or downward jumps of constant amplitudes a_+ and a_- take place. Let us recall that the Ornstein Uhlenbeck process $X = \{X_t, t \geq 0\}$ is the solution of the following stochastic differential equation

$$\begin{aligned} dX_t &= \left(-\frac{1}{\theta}X_t + \mu\right) dt + \sigma dW_t \\ X_0 &= X_{\text{rest}}. \end{aligned} \tag{2}$$

In this paper we consider the process N^- a Poisson process of intensity λ^-, i.e. with inter-events distributed as Exponential random variables of parameter λ^-. While we assign to the process N^+ different inter-events probability distributions, namely the followings:

1. inter-events distributed according to the random variable T^{IG}, Inverse Gaussian of parameters $(S_{\text{IG}}/\mu_{\text{IG}}, S_{\text{IG}}^2/\sigma_{\text{IG}}^2)$ with probability density function
$$g_{\text{IG}}(t) = \frac{S_{\text{IG}}}{\sqrt{2\pi t^3}\sigma_{\text{IG}}} \exp\left[-\frac{(S_{\text{IG}} - \mu_{\text{IG}} t)^2}{2\sigma_{\text{IG}}^2 t}\right] \tag{3}$$
2. inter-events distributed according to the random variable T^{OU}, first passage time of an Ornstein Uhlenbeck process (2) of parameters $(\mu_{\text{OU}}, \theta_{\text{OU}}, \sigma_{\text{OU}})$. The probability density function of the random variable T^{OU} is not known in closed form, but it can be simulated.
3. inter-events distributed according to the random variable T^{Γ}, given by
$$T^{\Gamma} = \begin{cases} T_1^{\Gamma} \sim \text{ Gamma } (\alpha_1, \beta_1) & \text{with probability 0.5,} \\ \\ T_2^{\Gamma} \sim \text{ Gamma } (\alpha_2, \beta_2) & \text{with probability 0.5.} \end{cases} \tag{4}$$

4. inter-events distributed according to the random variable T^{NET}, first passage time of a jump diffusion process V_{NET} given by (1) where the processes N^+ and N^- are both independent Poisson processes of parameters $\lambda^+_{\text{NET}}$and λ^-_{NET}.

After each crossing of the threshold S the process V is reset to $V_0 + N^+_T + N^-_T$, where T is the time of occurrence of the crossing. This means that the counting processes are not reset to N^+_0 and N^-_0 after the crossings of the threshold and that the spike train generated by (1) is not a renewal process [4].

Interpretation of the equations. The jump diffusion model (1) above introduced describes the membrane potential of the nerve cell evolving in time according to the depolarization and hyperpolarization caused by the inputs the cell receives. The weak and many inputs arriving from the network in which the cell is embedded are summed together in the continuous part of the process V. On the other hand the strong and few inputs that have a large impact on the membrane potential are treated separately and described by the two counting processes N^+ and N^-. Figure 1-a gives a graphical interpretation of model (1). The membrane potential of the cell A is given by the jump diffusion process V, obtained summing together weak inputs arriving from the network surrounding cell A (the arrows in Fig. 1-a) and strong inputs coming from an excitatory unit, cell E, and an inhibitory unit, cell I. The original formulation of the model

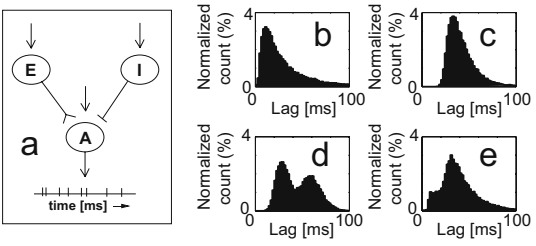

Fig. 1. Model (1) describes the membrane potential of the cell A, as the sum of the inputs arriving from the surrounding network, the excitatory unit E and the inhibitory unit I (panel a). Interspike interval histogram of the spike train of cell E when distributed as T^{IG} (panel a), T^{OU} (panel b), T^{Γ} (panel c) and T^{NET} (panel d).

arrives to equation (1) from Stein's model, and inherit from there the two counting processes N^+ and N^- Poisson distributed. We analyzed such case deep in details in [4]. There we found that as the frequency of the inhibitory strong inputs, λ^-, increases, the efficiency of the excitatory unit E, i.e. the number of spikes in the spike train of the cell E that excite cell A, increases too. In this paper we are interested in understanding whether this result is due to the Poisson distribution of the counting process N^+, that gives the times of firing of the cell E, or if it can be generalized to other distributions. For that reason we choose four different distributions of the events in the process N^+, T^{IG}, T^{OU}, T^{Γ}

and T^{NET}, and for each of them we study the excitatory efficiency of unit E on the cell A as the inhibitory frequency λ^- increases. Each one of the excitatory interevents distribution has been chosen for the properties of the spike train it generates. In Figure 1 the ISI histograms of the cell E when the intervents are distributed according to T^{IG} (panel b), T^{OU} (panel c), T^{Γ} (panel d) and T^{NET} (panel e) are plotted. We choose T^{IG} in order to make the cell E firing with ISIs distribution with very large variance, while we choose T^{OU} so that cell E fires with large refractory period (with no short lags). Moreover we chose T^{Γ} and T^{NET} because they make cell E firing with bimodal ISIs distribution. When we choose T^{Γ}, cell E fires with two well distinct and randomly merged characteristic times (the two modes of the histogram). On the other hand, when we consider T^{NET}, cell E fires with two characteristic times, the shorter one of them much less frequent than the larger one. Let us underline that the interspike intervals in Fig. 1-e correspond to the output of a small network (cf. Fig. 1-a). This fact induces correlations between successive spikes that are absent when the excitatory spikes come from the bimodal distribution T^{Γ} (cf. Fig. 1-d).

3 Results

The study of the model (1) is performed in two steps.

First of all the spike train of the cell A is simulated. To this purpose we had to adapt the classical techniques to simulate diffusion processes (cf. [2]) to the simulation of jump diffusion processes (cf. [4]). Concerning the simulation of the spike trains of the cells E and I, we proceed with suitable methods in each case. The generation of pseudo-random numbers Exponentially distributed and Gamma(α, β) distributed is trivial thanks to the classical method of inverse transformation of a uniformly distributed pseudo-random number. While to generate pseudo-random numbers Inverse Gaussian distributed we follow a method for inverse transformations with multiple roots (cf. [4]). Finally, to generate the spike train of the cell E when the inter-events are distributed as T^{NET}, we have to simulate them running the same algorithm that produces the firing times of the cell A, but with N^+ and N^- Poisson distributed.

The study of the simulated spike trains of the cells A, E, and I is performed plotting histograms of the interspike interval (ISI) distribution of the cell A and with the analysis of the autocorrelation and crosscorrelation histograms of the three cells. To plot autocorrelograms and crosscorrelograms we follow the method proposed by [1] using the program available at *http://openAdap.net/*. For each distribution of the excitatory unit E, we plot the excitatory efficiency as a function of the parameter λ^-, where we define excitatory efficiency the number of events in the spike train of the cell E that excite cell A (provoking its discharge). To evaluate such number of events we calculate the area of the peak around the lag zero above the upper confidence limit in the crosscorrelation histograms between cells A and E.

The threshold level is fixed at $S = 10$ mV with $V_0 = 0$ mV and the jump amplitudes are $a_+ = -a_- = 5$ mV. The values of the parameters of the continuous part

of process V are fixed as $\mu = 0.98$ mVms^{-1}, $\theta = 10$ ms and $\sigma^2 = 0.05$ mV^{2}ms^{-1}. The parameter μ cannot be directly interpreted from a biological point of view. We choose a value such that $\mu\theta < S$. This inequality defines the so called subthreshold regime of the Ornstein Uhlenbeck process, meaning that the process crosses the threshold just thanks to the random component W. Finally, in order to have a biologically compatible frequency of firing of the cell A, the value of σ is fixed as stated above. The parameter of the inhibitory frequency of firing varies from $\lambda^- = 10$ to $\lambda^- = 30$ ev/s. On the other hand the parameters of the excitatory distributions are chosen such that the frequency of firing of the cell E is always maintained in the range $[20 \text{ ev/s}, 30 \text{ ev/s}]$.

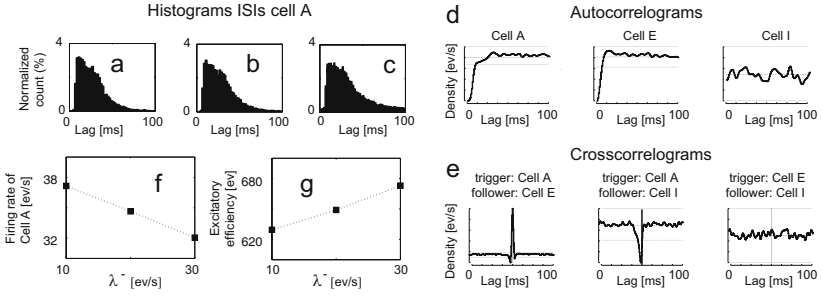

Fig. 2. Analysis of model (1) when the excitatory interspike intervals are T^{IG} distributed. ISIs histograms of cell A for $\lambda^- = 10$ (panel a), $\lambda^- = 20$ (panel b) and $\lambda^- = 30$ ev/s (panel c). Autocorrelation histograms of cells A, E and I (panel d) and crosscorrelation histograms of the cells (A,E), (A,I) and (E,I) for $\lambda^- = 20$ ev/s (panel e). Firing rate of cell A as a function of λ^- (panel f) and excitatory efficiency as a function of λ^- (panel g).

Excitatory Intervents T^{IG} distributed. Let us fix the parameter of the Inverse Gaussian distribution as follows: $S_{\text{IG}} = 10$ mV, $\mu_{\text{IG}} = 0.3$ mVms^{-1} and $\sigma^2_{\text{IG}} = 3$ mV^{2}ms^{-1}. So that we obtain an excitatory spike train that fires with large variance and also for relatively short lags.

The results are illustrated in Fig. 2. In panels a-b-c the ISI histograms of cell A are plotted as λ^- increases. No significant differences are appreciable from the histograms. The analysis of crosscorrelation histograms (cf. Fig. 2-g) shows that the excitatory efficiency increases as λ^- increases (so that cell A is more inhibited and its firing frequency decreases, cf. Fig. 2-f).

Excitatory Intervents T^{OU} distributed. Let us fix the parameter of the Ornstein Uhlenbeck distribution of the excitatory events as follows: $\mu_{\text{OU}} = 0.98$ mVms^{-1}, θ_{OU} ms and $\sigma^2_{\text{OU}} = 0.05$ mV^{2}ms^{-1}. So that we obtain an excitatory spike train that fires with relatively large lags and a large refractory period.

The results are illustrated in Fig. 3. In panels a-b-c the ISI histograms of cell A are plotted as λ^- increases. The ISI distribution is distinctly bimodal and the first peak loses probability mass as the cell A is more inhibited. The analysis

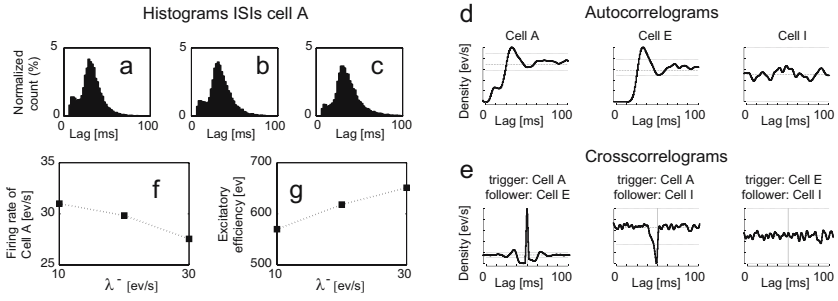

Fig. 3. Analysis of model (1) when the excitatory interspike intervals are T^{OU} distributed. ISIs histograms of cell A for $\lambda^- = 10$ (panel a), $\lambda^- = 20$ (panel b) and $\lambda^- = 30$ ev/s (panel c). Autocorrelation histograms of cells A, E and I (panel d) and crosscorrelation histograms of the cells (A,E), (A,I) and (E,I) for $\lambda^- = 20$ ev/s (panel e). Firing rate of cell A as a function of λ^- (panel f) and excitatory efficiency as a function of λ^- (panel g).

of crosscorrelation histograms (cf. Fig. 3-g) shows that the excitatory efficiency increases as λ^- increases (so that cell A is more inhibited and its firing frequency decreases, cf. Fig. 3-f).

Excitatory Intervents T^{Γ} distributed. Let us fix the parameter of the two Gamma distributions that build T^{Γ} as follows: $\alpha_1 = 30$, $\beta_1 = 0.5$ and $\alpha_2 = 15$, $\beta_2 = 0.5$. So that we obtain an excitatory spike train that fires with two characteristic times, the two modes of the ISI distribution of the excitatory spike train respectively (cf. Fig. 1-c).

The results are illustrated in Fig. 4. In panels a-b-c the ISI histograms of cell A are plotted as λ^- increases. The ISI distribution is weakly bimodal and the tail gains probability mass as the cell A is more inhibited. The analysis of crosscorrelation histograms (cf. Fig. 4-g) shows that the excitatory efficiency increases as λ^- increases (so that cell A is more inhibited and its firing frequency decreases, cf. Fig. 4-f).

Excitatory Intervents T^{NET} distributed. Let us fix the parameter of the process V_{NET} as follows: $S_{\mathrm{NET}} = 10$ mV and $a_+^{\mathrm{NET}} = -a_-^{\mathrm{NET}} = 5$ mV, $\mu_{\mathrm{NET}} = 0.98$ mVms^{-1}, $\theta_{\mathrm{NET}} = 10$ ms and $\sigma^2_{\mathrm{NET}} = 0.05$ mV^{2}ms^{-1} and $\lambda^+_{\mathrm{NET}} = \lambda^-_{\mathrm{NET}} = 10$ ev/s. So that we obtain an excitatory spike train that fires with two characteristic times, with the shorter lag that is less frequent rather than the larger one (cf. Fig. 1-d).

The results are illustrated in Fig. 5. In panels a-b-c the ISI histograms of cell A are plotted as λ^- increases. The ISI distribution is weakly bimodal and the tail gains probability mass as the cell A is more inhibited. Notice that the excitatory input ISI distribution is very similar to the ISI distribution of the cell A. The analysis of crosscorrelation histograms (cf. Fig. 5-g) shows that the excitatory efficiency increases as λ^- increases (so that cell A is more inhibited and its firing frequency decreases, cf. Fig. 5-f).

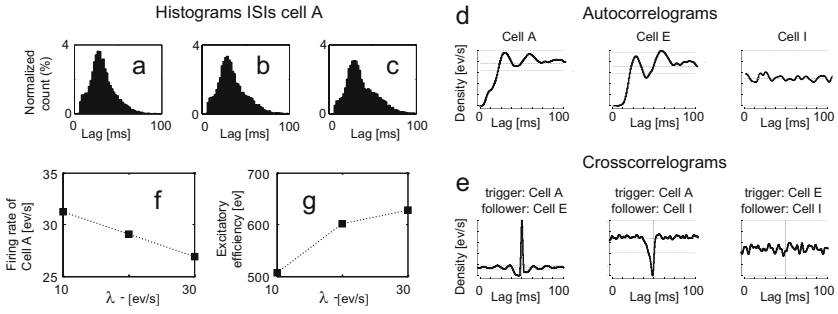

Fig. 4. Analysis of model (1) when the excitatory interspike intervals are T^{Γ} distributed. ISIs histograms of cell A for $\lambda^- = 10$ (panel a), $\lambda^- = 20$ (panel b) and $\lambda^- = 30$ ev/s (panel c). Autocorrelation histograms of cells A, E and I (panel d) and crosscorrelation histograms of the cells (A,E), (A,I) and (E,I) for $\lambda^- = 20$ ev/s (panel e). Firing rate of cell A as a function of λ^- (panel f) and excitatory efficiency as a function of λ^- (panel g).

4 Discussion

We discussed here the results obtained in the study of models (1) as the frequency of firing of the inhibitory unit I increases, and for different choices of interevents distribution of the excitatory spike train of unit E.

We selected four different probability distributions we denoted as T^{IG}, T^{OU}, T^{Γ} and T^{NET}. Each one of such choices produces excitatory spike trains with specific features we were interested in and has different impact on the firing of cell A. Let us notice that when we choose T^{IG}, the cell A fires with unimodal ISIs histogram, while the other choices produce bimodal ISIs distributions, with more separated peaks in the case T^{OU} and more mixed peaks in the case T^{Γ}. Finally the choice T^{NET}, makes the cell A fire with ISIs distribution very similar to the ISIs distribution of the excitatory unit E. The examples discussed confirm that in the small network modeled with (1) the inhibitory cells play an active role in signal transmission. Indeed, despite the variety of dynamics exhibited, the response of cell A to the excitatory spikes from cell E, as the inhibitory effect from unit I increases, exhibit the same trend, i.e. the excitatory efficiency increases as the inhibitory frequency of firing increase (cf. Fig. 2-g, 3-g, 4-g and 5-g). In other words, the more the cell A is inhibited, the better it responds to excitatory inputs. Let us recall that we define excitatory efficiency the number of events in the spike train of the cell E that excite cell A provoking its discharge. This feature has been at first analyzed in [4], where in model (1) the two counting processes N^+ and N^- were considered both Poisson processes. We test here the robustness of such property with respect to changes of the excitatory distribution of firing. It is now possible to state that such feature is typical of model (1) in its general formulation and that it is not due to the particular choice of the

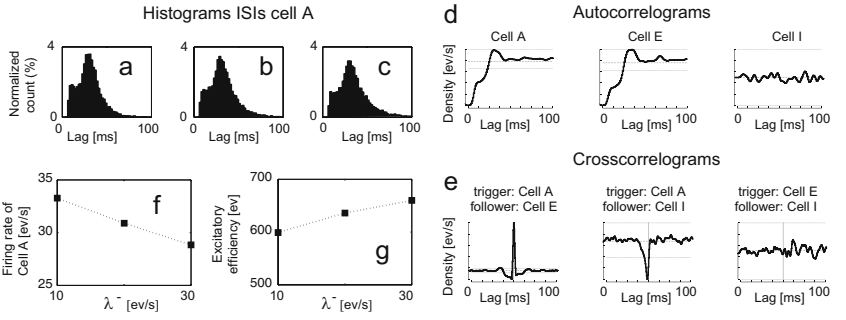

Fig. 5. Analysis of model (1) when the excitatory interspike intervals are T^{NET} distributed. ISIs histograms of cell A for $\lambda^- = 10$ (panel a), $\lambda^- = 20$ (panel b) and $\lambda^- = 30$ ev/s (panel c). Autocorrelation histograms of cells A, E and I (panel d) and crosscorrelation histograms of the cells (A,E), (A,I) and (E,I) for $\lambda^- = 20$ ev/s (panel e). Firing rate of cell A as a function of λ^- (panel f) and excitatory efficiency as a function of λ^- (panel g).

excitatory distribution performed in the previous work. Moreover we can state that such property is connected to the internal structure of the model and to the composition of a continuous diffusive part of the model with the strong discontinuities produced by the counting processes. From a biological point of view we could say that the superposition of stimuli of different intensities (i.e. weak and very frequent ones with strong and less numerous ones) can facilitate the neuronal transmission of the excitatory signal. In particular more important inhibitory stimulation makes the cell more efficient in responding to excitatory inputs. Such result, here tested in a larger validity, confirms the hypothesis that inhibitory neuronal cells may have a relevant role in neuronal coding and in information transmission, rather than only in keeping a balance of firing in the brain.

References

1. Abeles, M.: Quantification, smoothing and confidence limits for single units' histograms. J. Neurosci. Meth. 5, 317–325 (1982)
2. Kloeden, P.E., Platen, E.: Numerical solution of stochastic differential equations. In: Applications of Mathematics, vol. 23, Springer-Verlag, Heidelberg (1992)
3. Musila, M., Lánský, P.: Generalized Stein's model for anatomically complex neurons. BioSystems 25, 179–191 (1991)
4. Sirovich, R.: Mathematical models for the study of synchronization phenomena in neuronal networks. Ph. D. Thesis (2006)